Analytica Chimica Acta 1269 (2023) 341428

Contents lists available at ScienceDirect

Analytica Chimica Acta

journal homepage: www.elsevier.com/locate/aca

Analytic procedure for the evaluation of copper intermetallic diffusion in electroplated gold coatings with energy dispersive X-ray microanalysis

Walter Giurlani [a,b,*], Fabio Biffoli [a], Lorenzo Fei [a], Federico Pizzetti [a], Marco Bonechi [a], Claudio Fontanesi [b,c], Massimo Innocenti [a,b,d,e,**]

[a] Department of Chemistry "Ugo Schiff", University of Florence, Via della Lastruccia 3, 50019, Sesto Fiorentino, (FI), Italy
[b] National Interuniversity Consortium of Materials Science and Technology (INSTM), Via G. Giusti 9, 50121, Firenze, (FI), Italy
[c] Department of Engineering 'Enzo Ferrari', University of Modena and Reggio Emilia, Via Vivarelli 10, 41125, Modena, Italy
[d] National Research Council-Organometallic Compounds Chemistry Institute (CNR-ICCOM), Via Madonna del Piano 10, 50019, Sesto F.no, (FI), Italy
[e] Center for Colloid and Surface Science (CSGI), Via della Lastruccia 3, 50019, Sesto F.no, (FI), Italy

HIGHLIGHTS

- New method for intermetallic diffusion coefficient determination with EDS analysis.
- Qualitative evaluation of colour changing after inter-diffusion.
- Qualitative evaluation of composition profile variation after inter-diffusion.
- The results found are useful for evaluating the performance of barrier layers.

GRAPHICAL ABSTRACT

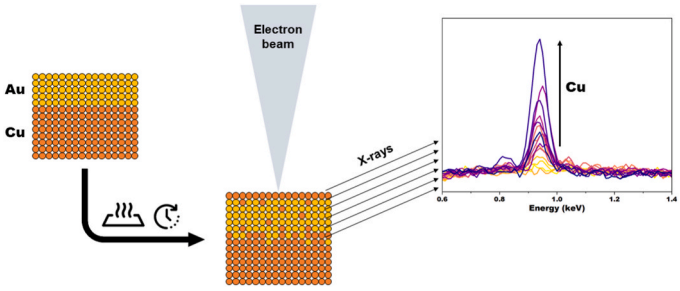

ARTICLE INFO

Handling Editor: Xiu-Ping Yan

Keywords:
Intermetallic diffusion
Electroplating
Energy dispersive X-ray spectroscopy
Gold copper system
Standardless

ABSTRACT

A method for the determination of the intermetallic diffusion coefficient in the Cu–Au system is described based on energy dispersive X-ray techniques. XRF and EDS analysis were used to measure the thickness of the electroplated gold coating and the copper diffused through it, respectively. This information was used to obtain the diffusion coefficient through an equation based on Fick's law. Colour measurements and metallographic section analysis of the samples were also performed to evaluate alternative methods for a qualitative determination of diffusion rate. The thickness of the gold layer was chosen in agreement with what is used in decorative and functional applications (<1 μm). The measurements were performed on samples heated in a range of temperatures between 100 °C and 200 °C from 12 to 96 h. The results obtained follow a linear trend between the logarithm of the diffusion coefficient and the inverse of the temperature and are in line with the values found in the literature.

* Corresponding author. Department of Chemistry "Ugo Schiff", University of Florence, Via della Lastruccia 3, 50019, Sesto Fiorentino, (FI), Italy.
** Corresponding author. National Interuniversity Consortium of Materials Science and Technology (INSTM), Via G. Giusti 9, 50121, Firenze, (FI), Italy.
E-mail addresses: walter.giurlani@unifi.it (W. Giurlani), m.innocenti@unifi.it (M. Innocenti).

https://doi.org/10.1016/j.aca.2023.341428
Received 8 February 2023; Received in revised form 3 May 2023; Accepted 24 May 2023
Available online 24 May 2023
0003-2670/© 2023 Elsevier B.V. All rights reserved.

1. Introduction

Electrodeposited gold-copper multiphase systems are widespread in many different industrial fields from electronics to decorative applications [1–3]. Specifically, in the high-fashion industry, common substrate materials are high percentage copper alloys like brass [3], moreover an electrodeposited copper layer is frequently used between the substrate and the finishing for its ability to reduce the small defects derived from mechanical polishing, the so called levelling power, providing high brightness to the final product [4]. Au–Cu systems aim to obtain cost effective artifacts that exploit the high conductivity and lower cost of copper and the chemical inertness of gold. One of the major problems of the Au–Cu systems is that separated copper and gold phases are not thermodynamically in equilibrium and intermetallic diffusion can occur, causing changes to important chemical-physical properties such as conductivity [5], corrosion resistance [6–9], topology [10] and colour [11–14]. The most important parameter that characterizes the intermetallic diffusion is the coefficient of diffusion D described by the Fick's first laws of diffusion (Eq. (1)).

$$F = -D\frac{dC}{dx} \tag{1}$$

where F is the diffusion flux in $mol \cdot m^2 \cdot s^{-1}$; D is the diffusion coefficient in $m^2 \cdot s^{-1}$; C is the concentration in $mol \cdot m^3$; x is the position in m.

The temperature variation of D can be modelled with the Arrhenius equation (Eq. 2) [15]. The linearity of the Arrhenius plot (log(D) vs 1/T, where T is the absolute temperature in K) is a strong indicator of the occurrence of a single diffusion mechanism and of the accuracy of the data [16].

$$D = D_0 e^{-\frac{E_A}{RT}} \tag{2}$$

where D_0 is the maximal diffusion coefficient in $m^2 \cdot s^{-1}$; E_A is the activation energy for diffusion in $J \cdot mol^{-1}$; R is the universal gas constant equal to 8.31446 J $(mol\ K)^{-1}$.

To preserve the characteristics of the products containing two metals with a high diffusion coefficient, a layer of a third metal, called barrier layer, must be placed between the two [17–19]. By choosing a metal with a low diffusion coefficient towards both other metals, diffusion can be limited. To select the most adequate barrier layer, the overall diffusion must be measured.

In solids, multiple diffusion mechanisms may occur depending on the measurement conditions and microstructure of the sample, among others lattice diffusion and grain boundary diffusion are the most common for metals [20]. Lattice diffusion, also known as bulk diffusion, is related to vacancy atoms exchanges and involves the diffusion between neighbouring planes of the diffusion matrix crystalline lattice [15]; this process is predominant at temperatures higher than $0.5 \cdot T_m \pm 20\%$, where T_m is the absolute melting temperature of the system [21]. Grain boundary diffusion, instead, is typical of polycrystalline materials and it is due to the diffusion between defects and pipes between grains. Grain boundary diffusion has a lower activation energy than lattice diffusion and is predominant at lower temperature [22]. The grain boundaries diffusion coefficient is strongly dependent on the geometry and compactness of the grains, the shape of the channels and can be strongly influenced by the deposition process [23–27]. More specifically, it has been observed it is influenced by the density of defects (such as dislocations) and the density and width of the pipes [23]. This last statement underlines the importance and the need, especially for the electroplating industry, to continue to study the intermetallic diffusion of gold-copper systems due the high variability of industrial electroplating processes and deposits. Then, depending on the temperature, three different kinetic mechanisms may been identified [21]: kinetics dominated by lattice diffusion ($T > 0.5 \cdot T_m$), mixed kinetics ($0.3 \cdot T_m < T < 0.5 \cdot T_m$) and kinetics dominated by diffusion through grain boundaries ($T < 0.3 \cdot T_m$). It is evident that in daily use plated objects are exclusively subjected to the latter.

It's important to highlight that intermetallic diffusion is a process also driven by law of mass action: at the interface between copper and gold a gradient in concentration is present with a slope more or less stiff depending on the time and the temperature to which the sample was subjected; then in the bulk of the gold layer the concentration of copper typically remains low; on the other hand, once copper reaches the surface, it will react with atmospheric oxygen causing the Cu^0 concentration on the outer surface to tend towards zero, drawing more copper from within the sample, resulting in most of the copper being on top of the gold surface as shown in (Fig. 1) [23,28]. Voids can also form at the interface of the two metals due to the Kirkendall effect [29–31]. This is a chemical-physical phenomenon which consists of the displacement of the interface between two metals due to the different speeds of diffusion of the atoms in the metals involved.

In electrodeposition industry, it is important to obtain the diffusion coefficient at the working temperature of the products [5], specifically room temperature for high-fashion industry. Diffusion coefficient determinations for AuCu systems at room temperature are extremally slow (more than 10 years per measure [28]), but they can be extrapolated from Eq. (1) obtained from fitting diffusion coefficients at higher temperature. To extrapolate valid data it is mandatory to select the temperature range to have the same diffusion kinetics for the desired temperature, specifically, for AuCu systems, grain boundary diffusion is prevalent at temperature below 250 °C [28].

In literature, there are various methods for determining the diffusion coefficient. Historically, the earliest works were based on the use of radioactive tracers [16,20,32]. This technique is limited to layers that are thick enough to be dissected to measure the amount of radioactive isotope concentration. In addition, it suffers from the impossibility of carrying out studies lasting longer than the half-life of the tracer [33]. Cross-sectioning and energy dispersive X-ray spectroscopy (EDS) microanalysis were also used to observe the migration of copper in gold coatings [30], but only samples with very thick layers (≈25 μm) were analysed. Subsequently, thanks mainly to the advent of new technologies, it became possible to perform low-temperature measurements, that need longer times, through various techniques. The most common depth profiling methods consist in coupling the sputtering of the surface of the sample with various surface analysis techniques such as Auger electron spectroscopy (AES) [22,23,28], X-ray photoelectron spectroscopy (XPS) [34], secondary ion mass spectrometry (SIMS) [22] or glow discharge optical emission spectrometry (GDOES) [17]. These more recent approaches (as opposed to the manual sectioning typical of the 1930s and 1950s) have opened the study of systems consisting of thin films, with sub-micron dimensionality, typical of the industrial applications. The conductivity monitoring was used to attempt to determine diffusion coefficients with electrical properties measurements: this methodology

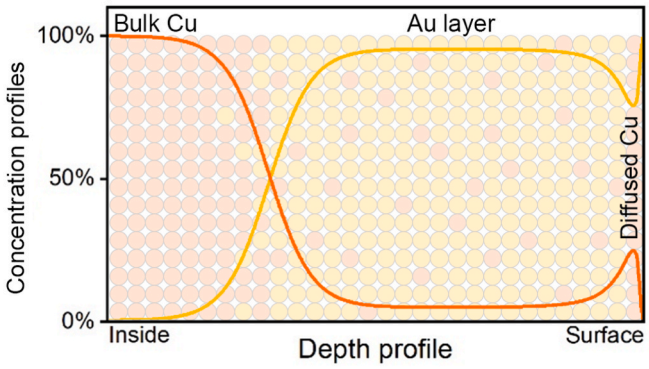

Fig. 1. Representation of the compositional profiles of a sample composed of a copper substrate and a gold coating. Image inspired by Ref. [23]. (For interpretation of the references to colour in this figure legend, the reader is referred to the Web version of this article.)

led to diffusion coefficients within ±10 cm^2/s compared to those determined with AES [28]. The main problem with the most accurate techniques listed above is that require highly specialized technical personnel and expensive instrumentations that are not common in most of the electronic and high-fashion industries, where intermetallic diffusion plays a key role. Lacking the right tools, in the decorative electroplating industry a very inexpensive colour-based qualitative method is adopted to determine if a finishing could run into problems due to intermetallic diffusion. The L × a*b × colorimetric coordinates of the specimen with the deposit of interest are measured with a colorimeter [35]; then the sample is placed in the oven for 24–48 h at 180 °C; once it has cooled down, the colour is remeasured, if it has not changed significantly the coating is approved. This method, although being very simple, does not give any idea of the diffusion coefficient and both time and temperature are chosen by pure convention.

The goal of this work is to propose and validate a novel methodology for the determination of intermetallic diffusion coefficients based on spectroscopic techniques affordable for industrial realities: EDS and X-ray fluorescence spectroscopy (XRF) [36]. Desktop scanning electron microscopes (SEM) equipped with EDS detector capable of the performances required in this study are already present in all the R&D laboratories of the electroplating baths suppliers, and their use also began to spread within production plants. XRF is even present in almost all the electroplating factories, and it is daily used for quality control to assess the thickness of deposited layers. For comparison the colour of the samples was also measured. The colorimeter is an instrument that is extremely widespread in many industries due to its affordability. For this reason we evaluate the possibility to use colorimeter to verify a correlation between the results.

2. Experimental

2.1. Samples preparation and characterization

Brass disks with a diameter of 2.5 cm were used as substrate. The samples were kindly prepared by electroplating companies (Italfimet Srl, AR, Italy and Materia Firenze Lab Srl, FI, Italy) on an industrial production line following a standard production process with proprietary commercial solutions: a thick deposit of copper (>20 μm) was electroplated on the substrates followed by a flash deposition (<50 nm) of a high carat gold-cobalt (>23.5 kt), then a pure gold (>99.9%) coating was deposited. The electrodeposition parameters of the final pure gold coating were adjusted to obtain a thickness approximately of 0.7 μm for each sample.

The samples were characterized before and after a thermal treatment performed at 100 °C, 135 °C, 170 °C and 200 °C for a time of 12, 24, 48 and 96 h, for a total of 16 samples (Table S1). After being washed with acetone, ethanol and water, the samples were placed in a covered glass Petri dish inside a Binder ED 115 oven with an electronic temperature control of ±1 °C. The Petri dish avoided gross particle contamination in the oven but was not an airtight seal, allowing air to pass in and out freely.

The characterizations involved the measurement of colour with a Konica Minolta (Tokyo, Japan) CM-700 d portable spectrophotometer using the specular component included (SCI) mode, 10° observer, D65 standard illuminant, and averaging the value of five measurements acquired in the centre of the sample.

X-ray fluorescence measurements (XRF) were performed with a Bowman BA-100 XRF spectrometer (Schaumburg, IL, USA), for the determination of the thickness of the gold coatings using the conventional fundamental parameter (FP) analysis corrected with a standard [37–39]. The following conditions were used: accelerating voltage of 50 kV, 0.8 mA current, 0.5 mm filter of aluminium and a collimator of 0.6 mm in diameter.

SEM images and microanalysis were obtained with variable pressure Hitachi SU3800 equipped with an Oxford Instruments NanoAnalysis Ultim Max 40 silicon drift EDS detector. The analysis was performed in the centre of sample surface using three different accelerating voltages: 5 kV, 10 kV and 20 kV. Low magnification (×200) was used to minimize the contribution of local inhomogeneities, the analysed area measured approximately 0.3 mm^2. The software CASINO v2.51 [40,41] was used to simulate and evaluate the penetration of the electrons and the depth of generated X-ray during the EDS analysis, the simulation was performed using 10^6 electrons with the various accelerating voltages. NIST DTSA-II Microscopium software [42–44] was used to simulate EDS spectra the evaluation of the equivalent thickness of copper migrated on the surface. The K–ratio method [45–47] was employed for this purpose, it is based on a semiquantitative approach that makes use of simulated calibration curves that only needs a mid-range desktop computer and can be used for the determination the nanometric and sub-nanometric thicknesses that would be expected from an equivalent diffused layer. The EDS spectra of layers with various thickness of copper (0.01, 0.02, 0.04, 0.08, 0.16, 0.32, 0.64, 1.20, 2.5, 5.00 nm) on a gold substrate was simulated using $32{\cdot}10^3$ electrons with an accelerating voltage of 5 kV, 10 kV, and 20 kV.

After all the surface analysis, the metallographic cross section of the samples was prepared, following a standard procedure [36], to perform an EDS profile analysis on the cross-section. The samples were protected by electrodepositing a layer of nickel; cut in half with a cut of machine; embedded in epoxy resin; polished with sanding paper degreasing the grain size and lapped with diamond suspension; the surface was carbon coated before the analysis.

2.2. Method for the determination of the diffusion coefficient

The proposed methodology uses Tompkins model [23] to calculate the coefficient diffusion, approximating Eq. (1) to Eq. (3). In this approximation the differentials dC and dx are converted in the differences ΔC and Δx; ΔC is calculated considering the concentration of copper is 0 on one side and the density of the metal on the other; Δx is the thickness of the gold layer; the flow *F* is obtained from the equivalent thickness of copper considering the density and the molar mass of the metal and diffusion time.

$$D = -\frac{F \bullet \Delta x}{\Delta C} = -\frac{\left(\frac{t_s \bullet \rho_s}{T \bullet M_s}\right) \bullet t_c}{\left(\frac{0-\rho_s}{M_s}\right)} = \frac{t_s \bullet t_c}{T} = \frac{t_{Cu} \bullet t_{Au}}{T} \quad (3)$$

where t_s (= t_{Cu}) is the equivalent thickness of the layer of the substrate, copper in our case, diffused on top of the coating, gold in this study; ρ_s is the density of the substrate; T is the period of time between two measurements; M_s is the molar mass of the substrate; t_c (= t_{Au}) is the thickness of the coating.

In his study Tompkins determined t_{Au} with an unspecified approximate method and t_{Cu} with AES measurements; in this study t_{Au} was obtained from XRF measurements and t_{Cu} with EDS measurements. The workflow of this method is schematized in the flowchart in Fig. 2.

3. Results and discussion

3.1. XRF thickness determination

The samples were characterized before and after the thermal annealing with XRF, SEM and colour measurements. First, the thickness of the gold coating (t_{Au}) was evaluated at the centre of the samples using XRF (Table S1). The results agreed with the expectations, with an average thickness of 0.696 ± 0.044 μm. Small variation was accepted as intrinsic to the deposition method. No significant variations were detected after annealing from the XRF measurement: the thickness values of gold remained the same, considering the instrument uncertainty, as well as the mean value 0.699 ± 0.052 μm. This result is justified by the high penetration of the high energy X-rays of the beam.

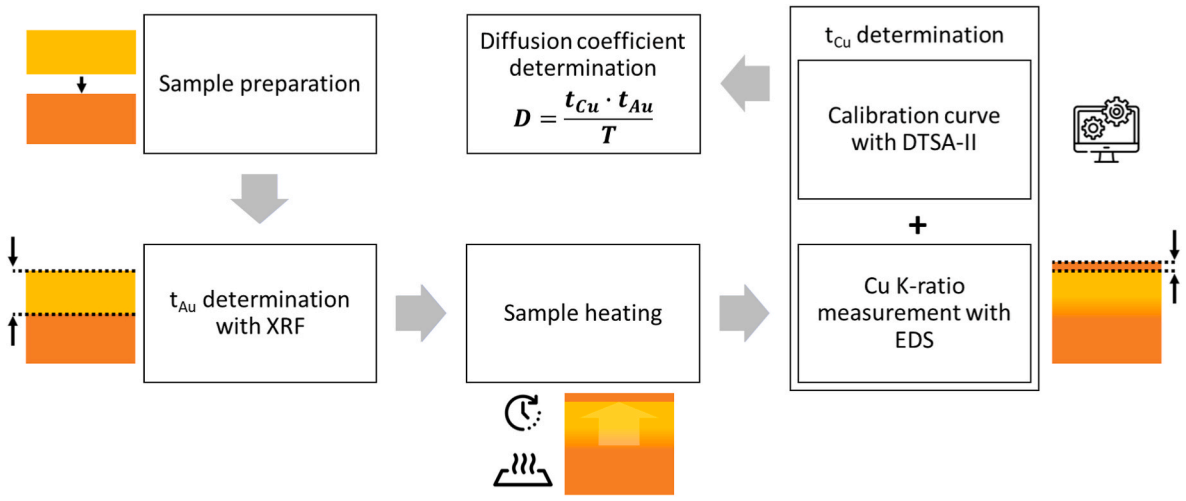

Fig. 2. Scheme of the workflow for the determination of the diffusion coefficient.

Even if any amount of copper diffused in the gold layer, or even onto the outer surface, the signal of gold does not change substantially.

3.2. Colour analysis

The main noticeable change in the samples following the annealing, in case copper diffusion through the gold layer up to the sample surface, should be the change in colour. German et al. [14] correlate the CIELAB colorimetric coordinates (L* brightness, a* green-red and b* blue-yellow) with the gold-silver-copper alloy composition. Based on their results L* and a × should not be greatly affected by the composition of gold-copper alloys while b × should change from a value larger than 30 for pure gold to a value lower than 15 for pure copper. Based on this evidence the colour of the samples was measured before and after the thermal treatment (Table S2).

In contrast to what expected the value of b × remained substantially unchanged in all samples. L* showed a slight decrease. While the a × values changed the most and showed some correlation with annealing time and temperature, although the results are scattered. Fig. 3 shows the variation of the a × value in terms of $\Delta a^* = a^*_{\text{Post-annealing}} - a^*_{\text{Pre-annealing}}$. Our hypothesis is that, for the times and temperatures used, copper migration mainly occurred through gold grain boundary channels without enough time to form an alloy, resulting in the presence of red copper on the sample surface. The use of a colorimetric measurement to evaluate the migration of copper, or of other metals, and therefore determine the effectiveness of a barrier layer would certainly be interesting at an industrial level due to its speed and simplicity. Unfortunately, the results show that with this method, it is only possible to obtain a qualitative evaluation, probably because colour variations can emerge due to the oxidation of contaminants present on the surface or of the metal itself.

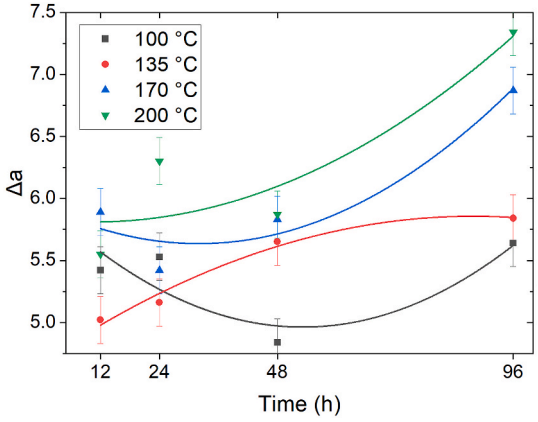

Fig. 3. Interaction plot of the variation in the colorimetric value a* ($\Delta a^* = a^*_{\text{Post-annealing}} - a^*_{\text{Pre-annealing}}$) as results of the thermal treatment. The different series correspond to the different annealing temperature investigated: black 100 °C; red 135 °C; blue 170 °C; green 200 °C. (For interpretation of the references to colour in this figure legend, the reader is referred to the Web version of this article.)

3.3. Surface microanalysis

The surface of the samples was compositionally characterized before and after the annealing with EDS using three different accelerating voltages: 5 kV, 10 kV and 20 kV. The microanalysis revealed only Au in the sample, before the annealing using 5 kV and 10 kV accelerating voltage, because the beam was not enough penetrating to pass the gold layer. Copper was detected in the spectra of the pre-annealed samples only using the accelerating voltage of 20 kV. After the annealing process copper was revealed also with the lower accelerating voltages confirming the diffusion of copper towards the surface (Fig. S1). The signal of copper was taken into consideration for further elaborations, in particular the K–ratio was used because it represents a raw information that can be extracted from the EDS spectrum (Table S3). The K–ratio is defined as the ratio in intensity of the same peak in the sample and in the standard, generally the pure element, measured in the same conditions. For the quantification, the L lines of Cu were used for the analysis performed at 5 kV and 10 kV, instead the K lines were exploited for the measurement at 20 kV.

The variation of the copper signal ($\Delta Cu = K\text{–ratio}_{\text{Post-annealing}} - K\text{–ratio}_{\text{Pre-annealing}}$) is reported in Fig. 4. The error bars were calculated by propagating the uncertainty of the K-ratio provided by the instrument, obtained by applying the Poisson distribution to the peak of interest. The measurement performed with 5 kV (Fig. 4a) shows the higher K–ratio variation and is evident the correlation between the signal and the annealing time as well the annealing temperature. The same considerations can be done using the 10 kV beam (Fig. 4b), but in this case the variation in the signal is lower, despite the noise in the EDS spectra is lower. The reason why the difference in the Cu K–ratio was lower for the 10 kV analysis is not fully clear. We suppose that, since after the annealing the concentration of Cu is higher on the surface of the sample (Fig. 1) and the 10 kV beam is more penetrating, the detected concentration of Cu is lower. A similar trend was observed also using the 20 kV beam, but in this case the interaction volume is even higher, and the Cu signal was detected also in the pre-annealed samples. Probably for this

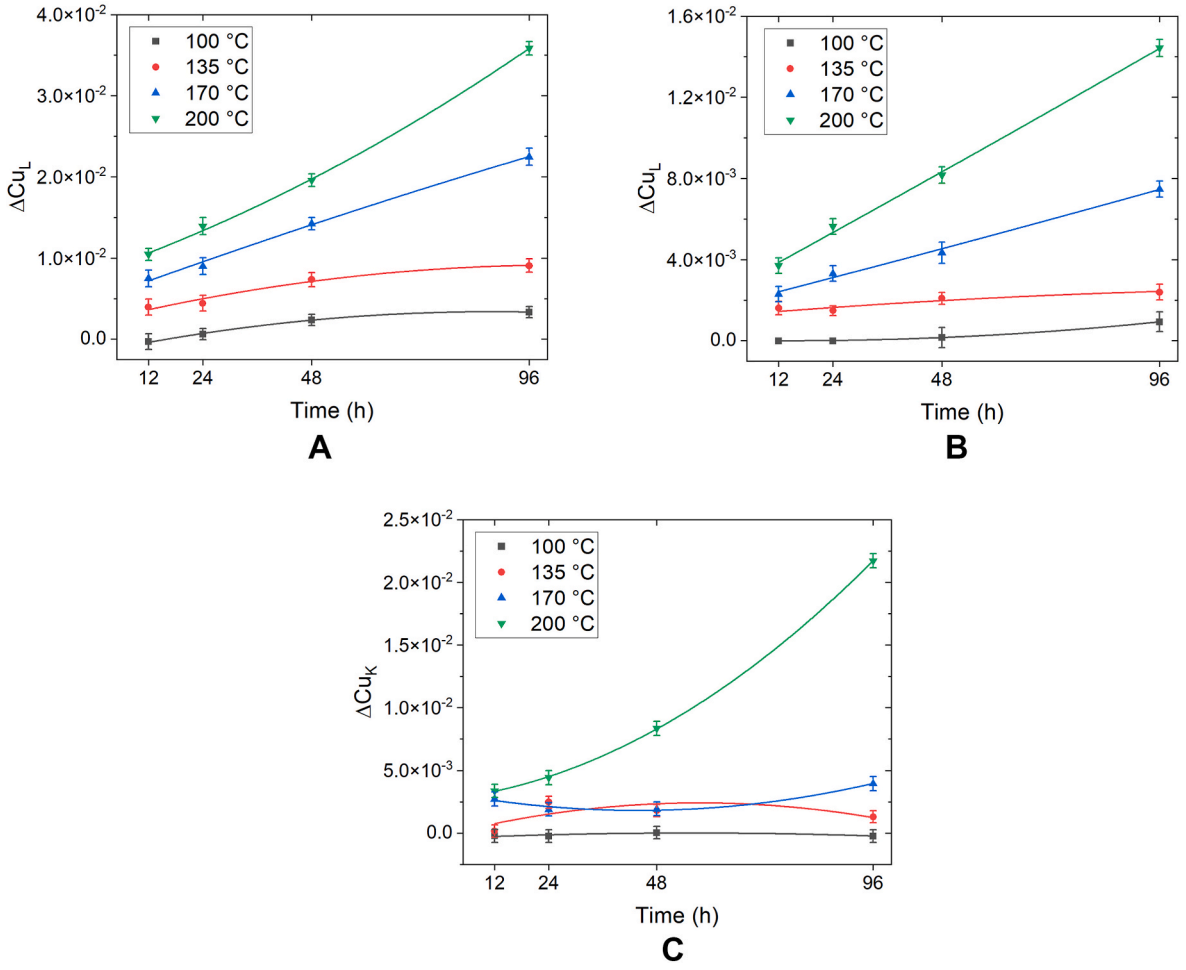

Fig. 4. Variation of the copper signal with EDS, performed with different accelerating voltage, as function of the annealing time: a) 5 kV; b) 10 kV; c) 20 kV. The different series correspond to the different annealing temperature investigated: black 100 °C; red 135 °C; blue 170 °C; green 200 °C. (For interpretation of the references to colour in this figure legend, the reader is referred to the Web version of this article.)

reason, the results are more scattered, and it is more difficult to evaluate the diffusion of the metal towards the surface. In each case the variation in signal is more evident using the higher temperature at a selected time or vice versa. For this reason, if a sample allows it, annealing at high temperature guarantees to observe results in a relatively short time, compatible with industrial standards. On the other hand, if a particular finish undergoes to deterioration at high temperatures (crimping, peeling, melting, etc.) or a different diffusion mechanism, the only option is to use longer times in order to obtain the same result.

From the results reported in Fig. 4, the electron beam with low penetration (5 kV) seems to provide better results. To evaluate the depth from where the X-ray of the EDS analysis were generated, a simulation using CASINO software (Fig. S2) was performed with an accelerating voltage of 5 kV. The result suggests that in a sample made of pure gold, the 99.9% of the signal (M emission) comes from the first 60 nm. Considering that in galvanic sector the coatings are generally higher than 100 nm, and often greater than 0.5 μm, this analysis can be considered as a surface characterization.

The next step was the evaluation of the diffusion coefficient D, considering the K–ratios obtained at 5 kV. DTSA-II software was used to simulate thin layers of copper with variable thickness on gold substrate. Then the K–ratios of the L emission line of copper were calculated for the simulated spectra, and the results were fitted with Eq. (4) to build the calibration curve (Fig. 5), used to convert the measured K–ratios in the equivalent thickness of Cu [45,48]. The curve fits the data points with an $R^2 > 0.9999$.

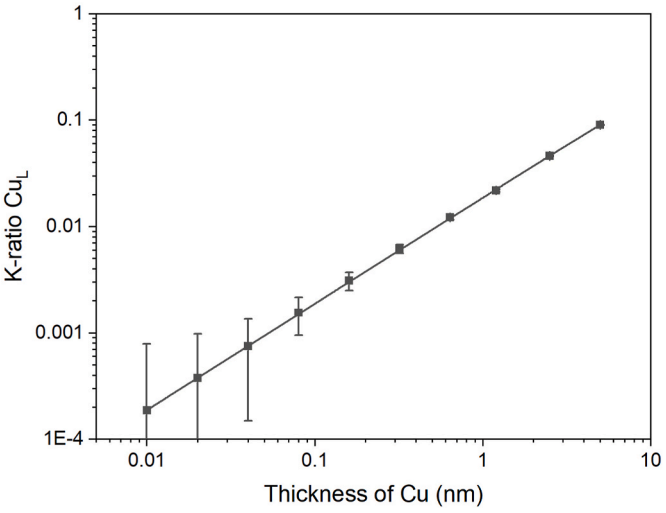

Fig. 5. Calibration curve obtained from EDS spectra simulated with DTSA-II and used to convert the measured K–ratios of the sample in the equivalent thickness of the diffused copper layer.

$$y = 1 - e^{-(Ax+Bx^2)} \quad (4)$$

The values of t_{Cu} are reported in Table 1. The samples 4, 8, 12 and 16, which are those heated for the longer time (96 h), have the lower relative uncertainty compared with the other samples heated at the same temperature. For this reason, these samples were considered for the determination of the diffusion coefficients and their representation in the Arrhenius plot.

3.4. Values of the diffusion coefficients obtained and comparison with literature

The values of D at a given temperature were calculated with Eq. (2) using the values of t_{Au}, obtained from XRF measurement, and the values of t_{Cu}, obtained from EDS measurements. The samples subjected to the longer heat treatment (samples 4, 8, 12 and 16 in Table S1) were considered because of their lower relative uncertainty. The results are reported in Table 2 and plotted in Fig. 6. The results obtained with the proposed methodology show a good linearity as it would be expected from the theoretical Arrhenius-like equation that describes the process. The linearity is a strong indicator of the accuracy of the data, and then of the methodology [16]. The Arrhenius plot of this work was compared with plots reported in literature on similar gold-copper systems and obtained with various methodologies: Campisano [49] studied a system with a thin layer (70 nm) of gold deposited by physical vapour deposition (PVD) on a copper substrate using the Rutherford backscattering spectrometry (RBS). Hall [22] measured the diffusion coefficient with AES analysis but information on how the samples were made is lacking. Hall [28] performed new measurements in 1977 on a variety of systems like PVD gold onto PVD copper; electrochemical deposition (ECD) of gold onto ECD copper; and ECD gold onto copper ribbons (ECD-R); the measurements included AES and conductimetry (COND). Tompkins [23] used AES analysis to perform measurements onto a system realized by electroplated copper covered by an electroplated strike layer (150 nm) of pure gold followed by a thick layer (25 μm) of electroplated cobalt-hardened gold. Raw data from Tompkins were taken, without the "actual diffusion area" correction whose determination is not well specified.

Values of D obtained with the proposed methodology, in addition to having excellent linearity, fall in the same range and have the same magnitude of the ones reported in literature. The main difference lies in the slope of the fitted lines, but this is strongly dependent by the deposition system [23] as it is related to the activation energy of the diffusion process [15,33]. For a better comparison with the literature data, the measurements were repeated on new samples prepared depositing pure gold directly on copper, without any AuCo layer, which was previously used to follow the industrial process. The diffusion coefficients were evaluated with the same methodology heating the samples for 96 h. The results are reported in Table 2 and plotted in Fig. 6. Even in this case the data show a good linearity in the Arrhenius plot. The fitted line has a higher slope if compared with the sample with the thin AuCo layer and is even more in agreement with literature data. This evidence confirms that this method can be used successfully in the evaluation of the performances of barrier layers.

Table 1
Thickness of the diffused copper layer, t_{Cu}, obtained from the calibration curve.

Sample	t_{Cu}	Sample	t_{Cu}
1	−0.02 ± 0.04	9	0.40 ± 0.05
2	0.03 ± 0.03	10	0.48 ± 0.05
3	0.13 ± 0.04	11	0.76 ± 0.04
4	0.18 ± 0.04	12	1.21 ± 0.06
5	0.21 ± 0.04	13	0.56 ± 0.04
6	0.24 ± 0.05	14	0.75 ± 0.05
7	0.40 ± 0.04	15	1.05 ± 0.04
8	0.49 ± 0.04	16	1.94 ± 0.05

Table 2
Diffusion coefficients obtained at different temperatures of AuCo and Cobalt-free samples.

Temperature (°C)	Diffusion coefficient $cm^2 \cdot s^{-1}$ ($\times 10^{17}$)	
	Cu/AuCo/Au	Cu/Au
100	0.3 ± 0.1	0.3 ± 0.5
135	1.0 ± 0.1	1.3 ± 0.5
175	2.4 ± 0.1	5.9 ± 0.8
200	4.1 ± 0.1	15 ± 1

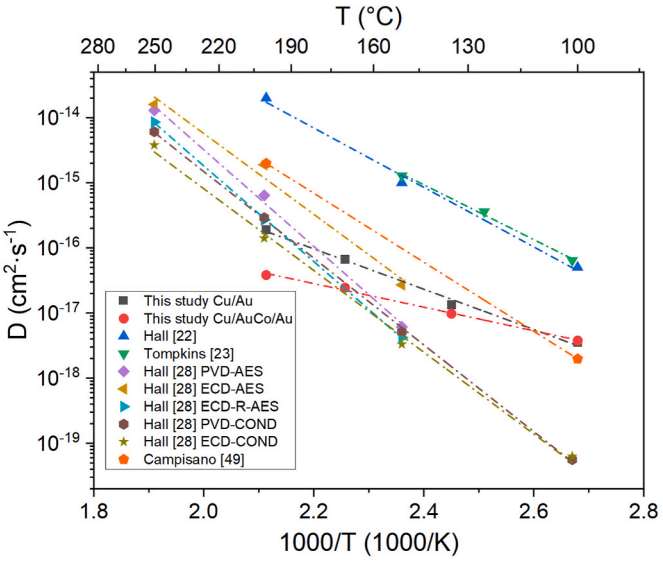

Fig. 6. Arrhenius plot for the diffusion coefficients of Au–Cu system obtained in this study and reported in literature.

Since even the presence of a thin layer containing a small percentage of cobalt can cause this variation, this confirms that the diffusion coefficient is strongly influenced by the growth conditions of the film, therefore the differences found in the literature are explained. Such differences are attributable to variations related to the microstructure of the deposited material and the deposition conditions. Samples prepared with different deposition techniques have resulted in different diffusion coefficients [28], because the structure of the deposit is related to the growth process [50], which also leads to differences in corrosion resistance [51]. For example, PVD is typically characterized by columnar growth that can lead to a steeper slope in the Arrhenius plot [52], compared to the electrodeposition method. Finally it should be noted that the formulations of electroplating solutions have undergone to many modifications over the last years, with the use of new electrolytes and additives [3]. Indeed, small changes in the composition of an alloy can significantly alter the microstructure of deposits and modifying intermetallic diffusion processes. Therefore, it is not easy to make a comparison even considering only electroplated samples. On the other hand, this suggests that by acting on deposition conditions it is possible to significantly limit the phenomenon of diffusion, and with the proposed approach, measuring the resulting differences would be easier.

3.5. SEM cross-section

Eventually, the metallographic cross sections of the samples were analysed with SEM-EDS. Fig. 7 shows the cross section of a sample at different magnification. It is possible to appreciate the brass substrate, the thick copper layer, the gold coating, and the nickel protection layer used for the cross sectioning. The white spots and bumps in the image are residues of the carbon coating process.

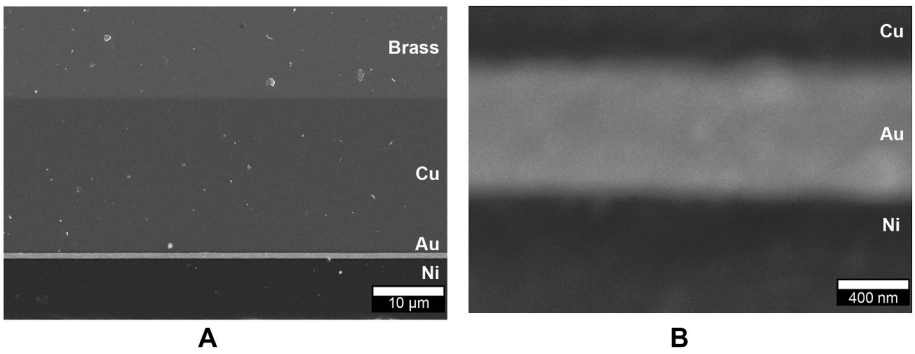

Fig. 7. Example of the SEM cross-section recorded at (a) low and (b) high magnification.

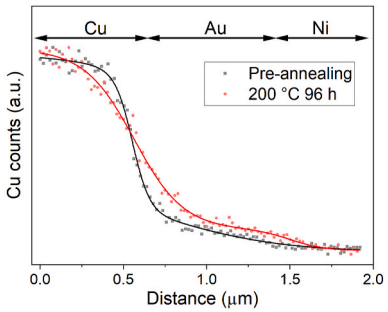

Fig. 8. Intensity of Cu L line measured along the profile of the cross section of a not-heated sample (black) and of the sample heated at the higher temperature (200 °C) for the longer time (96 h) (red). Guidelines have been added to assist the eye in interpreting the experimental data points. (For interpretation of the references to colour in this figure legend, the reader is referred to the Web version of this article.)

EDS profile analysis measurements were performed on all the cross sections. Fig. 8 reports the intensity of the signal of copper along the analysed profile, starting from the copper layer reaching up to the nickel layer. The overlap between a sample that has not been subjected to the thermal treatment and the sample heated at the higher temperature (200 °C) for the longer period (96 h) is reported. A difference can be discerned between the two profiles: the variation of the copper signal in the annealed sample is smoother as expected. Nevertheless, even though these samples represent the extreme conditions, the diffusion rate of copper is very hard to evaluate from these data. The causes can be found in the small thickness of the gold combined with the low lateral resolution of the EDS, which is a few hundred nanometres [36]. Pinnel [30] was able to detect Kirkendall porosity and even stoichiometric mixture of Cu_3Au and CuAu at the Cu–Au interface, using higher temperatures (250 °C) for much longer period (4 months) on very thick gold coatings (25 μm) finding a diffused layer of approximately 5.2 μm.

4. Conclusion

A method for the determination of intermetallic diffusion coefficient in the Cu–Au system by measuring the amount of copper emerged from gold coatings was described. The diffusion equation used in this study, derived from Fick's law of diffusion, exploits the thickness of the gold layer, the equivalent thickness of diffused copper, and the annealing time to evaluate the diffusion coefficient. The thickness of gold was measured with XRF and the thickness of copper with EDS. Compared to the literature lower temperatures, diffusion times and thickness of gold, which are compatible with the needs of the decorative and functional coatings industry, were used. Moreover, the instruments used, XRF and EDS, are more common, cheaper and more user friendly than the techniques used in the previous studies e.g., AES and XPS. The proposed method leads to results with a linear correlation between log(D) and T^{-1} and of the same order with the previously observed values.

Colour measurements of the samples and EDS microanalysis of the metallographic section were also carried out for the qualitative evaluation of the diffusion rate. In the first case a trend with the variation of the parameter a*, in the CIELAB colour space, was noticed, however a high dispersion of the results was found. In the second case the lateral resolution of the EDS was found to be insufficient for the gold thickness considered.

Considering the results obtained by coupling the XRF and EDS techniques, we expect that with the proposed approach it will be possible to study more easily the diffusion rates of many metals. Furthermore, it will be possible to design and implement new procedures for the realization of barrier layers against unwanted diffusion.

CRediT authorship contribution statement

Walter Giurlani: Conceptualization, Methodology, Validation, Formal analysis, Investigation, Writing – original draft, Visualization, Supervision, Project administration. **Fabio Biffoli:** Validation, Formal analysis, Investigation, Writing – original draft, Writing – review & editing. **Lorenzo Fei:** Investigation. **Federico Pizzetti:** Investigation. **Marco Bonechi:** Writing – review & editing. **Claudio Fontanesi:** Writing – review & editing. **Massimo Innocenti:** Writing – review & editing, Supervision, Project administration, Funding acquisition.

Declaration of competing interest

The authors declare that they have no known competing financial interests or personal relationships that could have appeared to influence the work reported in this paper.

Data availability

Data will be made available on request.

Acknowledgements

Italfimet Srl and Materia Firenze Lab Srl are acknowledged for making the samples used in this study.

Appendix A. Supplementary data

Supplementary data to this article can be found online at https://doi.org/10.1016/j.aca.2023.341428.

References

[1] S. Murali, N. Srikanth, C.J. Vath, An analysis of intermetallics formation of gold and copper ball bonding on thermal aging, Mater. Res. Bull. 38 (2003) 637–646, https://doi.org/10.1016/S0025-5408(03)00004-7.

[2] Y. Du, L.-Y. Gao, D. Yu, Z.-Q. Liu, Comparison and mechanism of electromigration reliability between Cu wire and Au wire bonding in molding state, J. Mater. Sci. Mater. Electron. 31 (2020) 2967–2975, https://doi.org/10.1007/s10854-019-02840-6.

[3] W. Giurlani, G. Zangari, F. Gambinossi, M. Passaponti, E. Salvietti, F. Di Benedetto, S. Caporali, M. Innocenti, F. Di Benedetto, S. Caporali, M. Innocenti, Electroplating for decorative applications: recent trends in research and development, Coatings 8 (2018) 260, https://doi.org/10.3390/COATINGS8080260, 8 (2018) 260.

[4] E. Bertorelle, Trattato di galvanotecnica, fourth ed., Hoepli, Milano, 2016. https://books.google.it/books?id=74DkjwEACAAJ.

[5] S.P. Pucic, Diffusion of copper into gold plating, in: 1993 IEEE Instrum. Meas. Technol. Conf., 1993, pp. 114–117, https://doi.org/10.1109/IMTC.1993.382669. IEEE.

[6] M. Mousavi, A. Kosari, J.M.C. Mol, Y. Gonzalez-Garcia, Localised aqueous corrosion of electroless nickel immersion gold-coated copper, Corrosion Eng. Sci. Technol. 57 (2022) 520–530, https://doi.org/10.1080/1478422X.2022.2096322.

[7] W. Giurlani, L. Sergi, E. Crestini, N. Calisi, F. Poli, F. Soavi, M. Innocenti, Electrochemical stability of steel, Ti, and Cu current collectors in water-in-salt electrolyte for green batteries and supercapacitors, J. Solid State Electrochem. 26 (2022) 85–95, https://doi.org/10.1007/s10008-020-04853-2.

[8] E. Berretti, N. Calisi, A. Capaccioli, L. Capozzoli, A.M.S. Hamouda, A. Giaccherini, W. Giurlani, A. Ienco, S. Martinuzzi, M. Innocenti, U. Waware, S. Virtanen, G. Zangari, R. Ahmed, A. Lavacchi, Electrodeposited white bronzes on brass: corrosion in 3.5 % sodium chloride solution, Corrosion Sci. 175 (2020), 108898, https://doi.org/10.1016/j.corsci.2020.108898.

[9] W. Giurlani, P. Marcantelli, F. Benelli, D. Bottacci, F. Gambinossi, M. Passaponti, A. De Luca, E. Salvietti, M. Innocenti, Corrosion resistance test of electroplated gold and palladium using fast electrochemical analysis, Coatings 9 (2019) 405, https://doi.org/10.3390/coatings9060405.

[10] R. Szczepaniak, Effect of surface topology on the apparent thermal diffusivity of thin samples at LFA measurements, Materials 15 (2022) 4755, https://doi.org/10.3390/ma15144755.

[11] O. Arnache, G. Ricaurte, J. Fabian-Salvador, H. Pimienta, Analytical approach of colour and elemental composition in gold metallic objects from the Quimbaya culture: a case study in Antioquia, Colombia, J. Archaeol. Sci. Reports. 42 (2022), 103290, https://doi.org/10.1016/j.jasrep.2021.103290.

[12] S.H. Hong, S.C. Mun, G.C. Kang, H.J. Park, Y.B. Jeong, G. Song, K.B. Kim, Recent development of coloring alloys, Prog. Mater. Sci. 123 (2022), 100811, https://doi.org/10.1016/j.pmatsci.2021.100811.

[13] A. Manas, Gold's red shift: colorimetry of multiple reflections in grooves, Gold Bull. 53 (2020) 147–158, https://doi.org/10.1007/s13404-020-00285-y.

[14] R.M. German, M.M. Guzowski, D.C. Wright, The colour of gold-silver-copper alloys, Gold Bull. 13 (1980) 113–116, https://doi.org/10.1007/BF03216549.

[15] M. Ohring, Kinetics of mass transport and phase transformations, in: Eng. Mater. Sci., Elsevier, 1995, pp. 249–297, https://doi.org/10.1016/B978-012524995-9/50030-1.

[16] D.B. Butrymowicz, J.R. Manning, M.E. Read, Diffusion in copper and copper alloys. Part I. Volume and surface self-diffusion in copper, J. Phys. Chem. Ref. Data 2 (1973) 643–656, https://doi.org/10.1063/1.3253129.

[17] D. Rossi, S. Ciappelli, J. Silert, Electroplated Product Having a Precious Metal Finishing Layer and Improved Corrosion Resistance, Method for its Production and Uses Thereof, WO2016166330A1, 2016.

[18] J. Pradhan, A. Sankarakumar, S.K. Srivastava, S. Balakrishnan, Study of inter-diffusion of gold in copper in the presence of single layer graphene, Surface. Interfac. 30 (2022), 101923, https://doi.org/10.1016/j.surfin.2022.101923.

[19] W. Shao, Y. Sun, W. Giurlani, M. Innocenti, G. Zangari, Estimating electrodeposition properties and processes: Cu-Ag alloy at n-Si(001) and Ru substrates from acidic sulfate bath, Electrochim. Acta 403 (2022), 139695, https://doi.org/10.1016/j.electacta.2021.139695.

[20] A.D. Le Claire, Diffusion in metals, Prog. Met. Phys. 4 (1953) 265–332, https://doi.org/10.1016/0502-8205(53)90019-7.

[21] D. Gupta, Diffusion in metallic thin films, Defect Diffusion Forum 59 (1991) 137–150. https://doi.org/10.4028/www.scientific.net/DDF.59.137.

[22] P.M. Hall, J.M. Morabito, A formalism for determining grain boundary diffusion coefficients using surface analysis, Surf. Sci. 59 (1976) 624–630, https://doi.org/10.1016/0039-6028(76)90041-8.

[23] H.G. Tompkins, M.R. Pinnel, Low-temperature diffusion of copper through gold, J. Appl. Phys. 47 (1976) 3804–3812, https://doi.org/10.1063/1.323265.

[24] E. Mariani, W. Giurlani, M. Bonechi, V. Dell'Aquila, M. Innocenti, A systematic study of pulse and pulse reverse plating on acid copper bath for decorative and functional applications, Sci. Rep. 12 (2022), 18175, https://doi.org/10.1038/s41598-022-22650-x.

[25] L. Fabbri, W. Giurlani, G. Mencherini, A. De Luca, M. Passaponti, E. Piciollo, C. Fontanesi, A. Caneschi, M. Innocenti, Optimisation of thiourea concentration in a decorative copper plating acid bath based on methanesulfonic electrolyte, Coatings 12 (2022) 376, https://doi.org/10.3390/coatings12030376.

[26] W. Giurlani, M. Vizza, F. Pizzetti, M. Bonechi, M. Savastano, L. Sorace, A. Stefani, C. Fontanesi, M. Innocenti, Magnetic field effect on the handedness of electrodeposited heusler alloy, Appl. Sci. 12 (2022) 5640, https://doi.org/10.3390/app12115640.

[27] F. Pizzetti, E. Salvietti, W. Giurlani, R. Emanuele, C. Fontanesi, M. Innocenti, Cyanide-free silver electrodeposition with polyethyleneimine and 5,5-dimethyl-hydantoin as organic additives for an environmentally friendly formulation, J. Electroanal. Chem. 911 (2022), 116196, https://doi.org/10.1016/j.jelechem.2022.116196.

[28] P.M. Hall, J.M. Morabito, N.T. Panousis, Interdiffusion in the Cu-Au thin film system at 25°C to 250°C, Thin Solid Films 41 (1977) 341–361, https://doi.org/10.1016/0040-6090(77)90320-0.

[29] P.G. Kotula, S.V. Prasad, Visualization of Kirkendall voids at Cu-Au interfaces by in situ TEM heating studies, J. Occup. Med. 71 (2019) 3521–3530, https://doi.org/10.1007/s11837-019-03708-0.

[30] M.R. Pinnel, Diffusion-related behaviour of gold in thin film systems, Gold Bull. 12 (1979) 62–71, https://doi.org/10.1007/BF03216542.

[31] K. WeiterhausS, W. Zhang-Beglinger, J. Guebey, Adhesion Promotion of Cyanide-free White Bronze, US20130236742A1, 2013.

[32] L. Slifkin, D. Lazarus, T. Tomizuka, The diffusion of antimony in silver single crystals, J. Appl. Phys. 23 (1952), https://doi.org/10.1063/1.1702151, 1405–1405.

[33] A.B. Martin, R.D. Johnson, F. Asaro, Diffusion of gold into copper, J. Appl. Phys. 25 (1954) 364–369, https://doi.org/10.1063/1.1721642.

[34] K. Asami, E. Akiyama, K. Hashimoto, XPS determination of diffusion coefficients of cations in thin passive films on alloys, Solid State Phenom. 72 (2000) 79–84. https://doi.org/10.4028/www.scientific.net/SSP.72.79.

[35] W. Giurlani, F. Gambinossi, E. Salvietti, M. Passaponti, M. Innocenti, Color measurements in electroplating industry: implications for product quality control, ECS Trans. 80 (2017) 757–766, https://doi.org/10.1149/08010.0757ecst.

[36] W. Giurlani, E. Berretti, M. Innocenti, A. Lavacchi, Measuring the thickness of metal coatings: a review of the methods, Coatings 10 (2020) 1211, https://doi.org/10.3390/coatings10121211.

[37] E. Scialla, J. Brocchieri, C. Sabbarese, Comparison of different methodologies for estimating gold thickness in multilayer samples using XRF spectra, Appl. Radiat. Isot. 191 (2023), 110517, https://doi.org/10.1016/j.apradiso.2022.110517.

[38] S. Martinuzzi, C. Giovani, W. Giurlani, E. Galvanetto, N. Calisi, M. Casale, C. Fontanesi, S. Ciattini, M. Innocenti, A robust and cost-effective protocol to fabricate calibration standards for the thickness determination of metal coatings by XRF, Spectrochim. Acta Part B At. Spectrosc. 182 (2021), 106255, https://doi.org/10.1016/j.sab.2021.106255.

[39] W. Giurlani, E. Berretti, A. Lavacchi, M. Innocenti, Thickness determination of metal multilayers by ED-XRF multivariate analysis using Monte Carlo simulated standards, Anal. Chim. Acta 1130 (2020) 72–79, https://doi.org/10.1016/j.aca.2020.07.047.

[40] D. Drouin, Casino (n.d.), https://www.gegi.usherbrooke.ca/casino/.

[41] D. Drouin, A.R. Couture, D. Joly, X. Tastet, V. Aimez, R. Gauvin, Casino V2.42—a fast and easy-to-use modeling tool for scanning electron microscopy and microanalysis users, Scanning 29 (2007) 92–101, https://doi.org/10.1002/sca.20000.

[42] N.W.M. Ritchie, Nist dtsa-II (n.d.), http://www.cstl.nist.gov/div837/837.02/epq/dtsa2/.

[43] D.E. Newbury, N.W.M. Ritchie, Simulating electron-excited energy dispersive X-ray spectra with the NIST DTSA-II open-source software platform, MRS Adv (2022), https://doi.org/10.1557/s43580-022-00300-8.

[44] D.E. Newbury, N.W.M. Ritchie, Energy-dispersive X-ray spectrum simulation with NIST DTSA-II: comparing simulated and measured electron-excited spectra, Microsc. Microanal. 28 (2022) 1905–1916, https://doi.org/10.1017/S1431927622012272.

[45] W. Giurlani, M. Innocenti, A. Lavacchi, X-Ray microanalysis of precious metal thin films: thickness and composition determination, Coatings 8 (2018) 84, https://doi.org/10.3390/coatings8020084.

[46] G.D. Pereyra, F.Y. Oliva, N. Budini, G. Risso, P.D. Pérez, S. Suárez, J.C. Trincavelli, Standardless determination of nanometric thicknesses in stratified samples by electron probe microanalysis, Spectrochim. Acta Part B At. Spectrosc. 171 (2020), 105932, https://doi.org/10.1016/j.sab.2020.105932.

[47] L. Fabbri, W. Giurlani, F. Biffoli, M. Bellini, H. Miller, C. Fontanesi, F. Vizza, M. Innocenti, Exploiting the combination of displacement and chemical plating for a tailored electroless deposition of palladium films on copper, Appl. Sci. 11 (2021) 8403, https://doi.org/10.3390/app11188403.

[48] C.S. Campos, E.A. Coleoni, J.C. Trincavelli, J. Kaschny, R. Hubbler, M.R.F. Soares, M.A.Z. Vasconcellos, Metallic thin film thickness determination using electron probe microanalysis, X Ray Spectrom. 30 (2001) 253–259, https://doi.org/10.1002/xrs.495.

[49] S.U. Campisano, G. Foti, F. Grasso, E. Rimini, Determination of concentration profile in thin metallic films: applications and limitations of He+ backscattering, Thin Solid Films 25 (1975) 431–440, https://doi.org/10.1016/0040-6090(75)90061-9.

[50] J.L. Daure, M.J. Carrington, P.H. Shipway, D.G. McCartney, D.A. Stewart, A comparison of the galling wear behaviour of PVD Cr and electroplated hard Cr thin films, Surf. Coating. Technol. 350 (2018) 40–47, https://doi.org/10.1016/j.surfcoat.2018.06.070.

[51] S.M. Martinuzzi, L. Donati, W. Giurlani, F. Pizzetti, E. Galvanetto, N. Calisi, M. Innocenti, S. Caporali, A comparative research on corrosion behavior of electroplated and magnetron sputtered chromium coatings, Coatings 12 (2022) 257, https://doi.org/10.3390/coatings12020257.

[52] P. Panjan, A. Drnovšek, P. Gselman, M. Čekada, M. Panjan, Review of growth defects in thin films prepared by PVD techniques, Coatings 10 (2020) 447, https://doi.org/10.3390/coatings10050447.